Multisensory strategies for postural compensation after lateral line loss

Samantha N. Davis [1], **Yunlu Zhu** [1], **David Schoppik** [1,2,*]
[1] Depts. of Otolaryngology, Neuroscience & Physiology, and the Neuroscience Institute, NYU Grossman School of Medicine
[2] Lead Contact
[*] Correspondence: schoppik@gmail.com

To control elevation underwater, aquatic vertebrates integrate multisensory information (e.g., vestibular, visual, proprioceptive) to guide posture and swim kinematics. Here we characterized how larval zebrafish changed posture and locomotive strategies after imposed instability (decreased buoyancy) in the presence and absence of visual cues. We discovered that larvae sank more after acute loss of lateral line (flow-sensing) hair cells. In response, larvae engaged different compensatory strategies, depending on whether they were in the light or dark. In the dark, larvae swam more frequently, engaging their trunk to steer their nose up and climb more effectively. However, in the light, larvae climbed more often, engaging both pectoral fins and trunk to elevate. We conclude that larvae sense instability and use vestibular and visual information as available to control posture and trajectory. Our work is a step towards understanding the multisensory neural computations responsible for control strategies that allow orientation and navigation in depth.

INTRODUCTION

Postural control and movement both use multisensory information about an organism's relationship to its environment. The vestibular system detects linear (e.g. gravity) and angular acceleration [1]; proprioception encodes body position and movement [2]; vision captures both position and direction relative to the world; and for fish, the lateral line senses flow [3]. Aquatic vertebrates leverage this multisensory data to orient and navigate in depth. For instance, fish can pitch upwards to direct thrust from the trunk [4,5]. In addition, most teleost fish use a gas filled organ called the swim bladder to regulate density [6,7]. Finally, during swimming, morphological asymmetries [8] or fin engagement [4] can generate lift to increase elevation. How multisensory input changes postural behaviors as fish climb and dive remains an open question.

A common laboratory model teleost, the larval zebrafish (*Danio rerio*), has opened a window into the mechanisms of elevation control [9]. First, because larvae swim in discrete bouts of translation [10] and do not glide in between bouts, it is straightforward to estimate the forces acting on their bodies. Recent work has leveraged this active/passive dichotomy to understand postural control in the pitch [11,12] and roll axes [13], as well as the pectoral fin and trunk contributions to climbing bouts [14]. Next, larvae inflate their swim bladders early [15–17], achieving near neutral buoyancy [18]. Prior work suggests that when this buoyancy is experimentally altered, larvae change their posture, swim frequency, and/or swim trajectories to compensate. Specifically, after decreases in buoyancy (oil-filled swim bladders) larvae (1) adopt more nose-up postures, which impose a compensatory vertical component to their translation, (2) climb more, and (3) move more frequently [11,19]. Similarly, after increasing relative buoyancy (adding glycerol to the water), larvae dive more often [19]. These manipulations are unhealthy and can only be maintained for short periods limiting all but cursory investigation.

Here, we illuminate multisensory strategies that larval zebrafish use to regulate elevation when challenged. After lateral line hair cell ablation, we observed that larvae sank profoundly more than control siblings. In response, larvae without lateral line hair cells swam more frequently in the dark. When they climbed, they relied on trunk rotations to ascend more effectively. In the light, however, larvae without lateral line hair cells climbed more often, and did so with a combination of fin lift and trunk rotation. We conclude that larvae sense positional instability and restore elevation using vestibular and visual information when available. Our work reveals the multisensory nature of the computations that larval zebrafish use to maintain their depth, and points the way forward to investigate neural substrates responsible for vertical navigation.

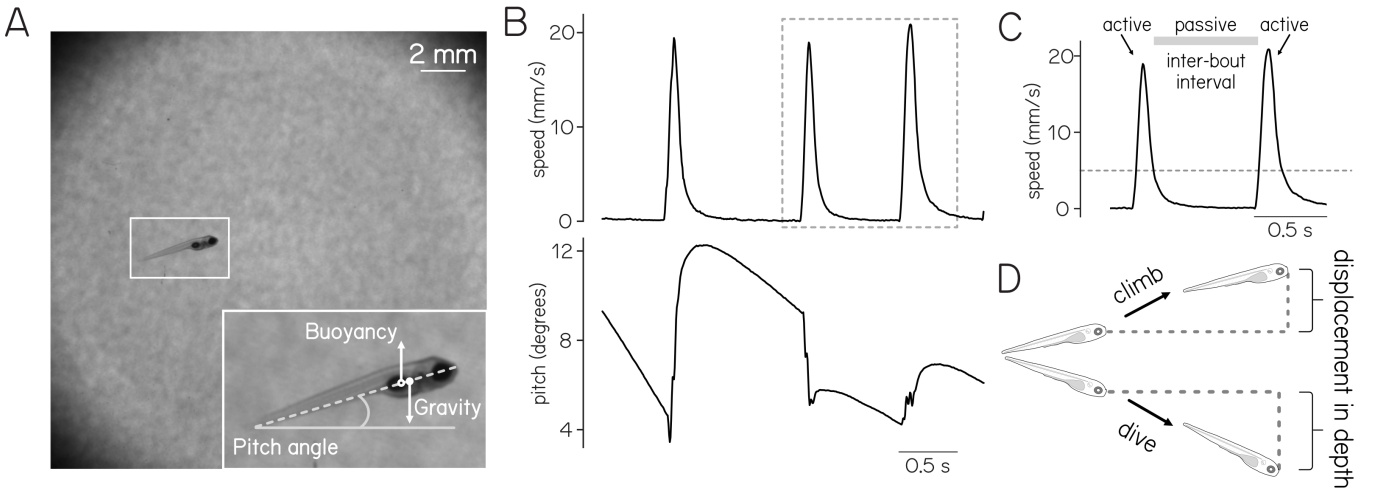

Figure 1: Physical forces and kinematic parameters of larval locomotion in the vertical plane.
(A) Example field of view (4 cm^2) with a 5 dpf larvae. Inset shows the pitch of the larvae, defined as the angle between the long axis of the body and the horizon; the gravity vector acting at the center of mass; and the buoyancy vector acting at the center of volume.
(B) Representative sequence of swim bouts, plotted as speed (top) and pitch (bottom) as a function of time. Positive values for pitch are nose-up.
(C) Schematic of two swim bouts illustrating the speed threshold (5 mm/s) that defines the active bout, as well as the passive inter-bout interval.
(D) Schematic of larvae at the beginning and end of a climb and dive bout, illustrating the vertical displacement.

RESULTS

Larvae compensate for postural instability after lateral line ablation

We used a videographic assay called SAMPL, or the Scalable Apparatus for Measuring Posture and Locomotion [12], to measure behavior. SAMPL consists of a rectangular arena designed to encourage depth exploration, a high-speed camera focused on the middle of the arena, and machine vision software to extract position and posture in the pitch (nose-up/nose-down) axis (Figure 1A) as a function of time. Larval zebrafish swim with short active bursts of translation called "bouts" (Figures 1B and 1C). During the inter-bout interval (Figure 1C), larvae are largely passive, allowing us to estimate the net effect of physical forces that challenge posture (i.e. gravity & buoyancy). Finally, larvae navigate in depth by adjusting posture during propulsive bouts to climb (nose-up) or dive (nose-down) (Figure 1D).

We selectively ablated lateral line hair cells by exposing larvae (7 days post-fertilization, or dpf) to ototoxic levels (10 μM) of copper sulfate ($CuSO_4$; shortened hereafter to "copper") for 90 minutes every 24 hours (Figure 2A) per established protocols [20,21]. Treatment produced rapid and complete loss of exposed lateral line hair cells (Figure 2B) while preserving inner ear vestibular hair cells, which are protected by the otic capsule. Using SAMPL, we monitored behavior in copper-treated larvae and control siblings for 24 hours before and 48 hours after copper exposure. All behavior was measured in complete darkness. Before treatment, all larvae showed comparable behavior (Table 1).

Copper-treated larvae sank considerably more than untreated siblings. Vertical displacement in depth during the inter-bout interval was greater in copper-treated larvae than untreated siblings (median [inter-quartile range]; -0.32 [0.63] mm vs. 0.02 [0.62] mm, p=0.0219, Figures 2C and 2D). Copper-treated larvae sank in the vertical axis far more quickly than untreated siblings (-0.32 [0.29] mm/s vs. -0.02 [0.43] mm/s, p=0.00928, Figures 2E and 2F). Sinking remained comparable across the duration of the experiment (Table 3), and could be observed during individual inter-bout intervals (Supplementary Video 1).

Copper-treated larvae swam more frequently and adopted a more nose-up pitch. Their inter-bout interval duration was significantly shorter than untreated siblings (1.45 [1.52] s vs. 1.78 [2.27] s, p=0.03405, Figures 2G and 2H). Additionally, their median posture was significantly more "nose-up" than untreated siblings (12.42 [16.81]° vs. 8.64 [17.64]°, p=0.001, Figures 2I and 2J). In the inter-bout interval, copper-treated larvae rotated nose-down more quickly compared to untreated siblings (-6.45 [3.68]°/s vs. -2.71 [3.69]°/s, p=4.6e-4, Figures 2K and 2L). Notably, we observed fewer total swim bouts in copper-treated larvae (n=13126 vs n=32713).

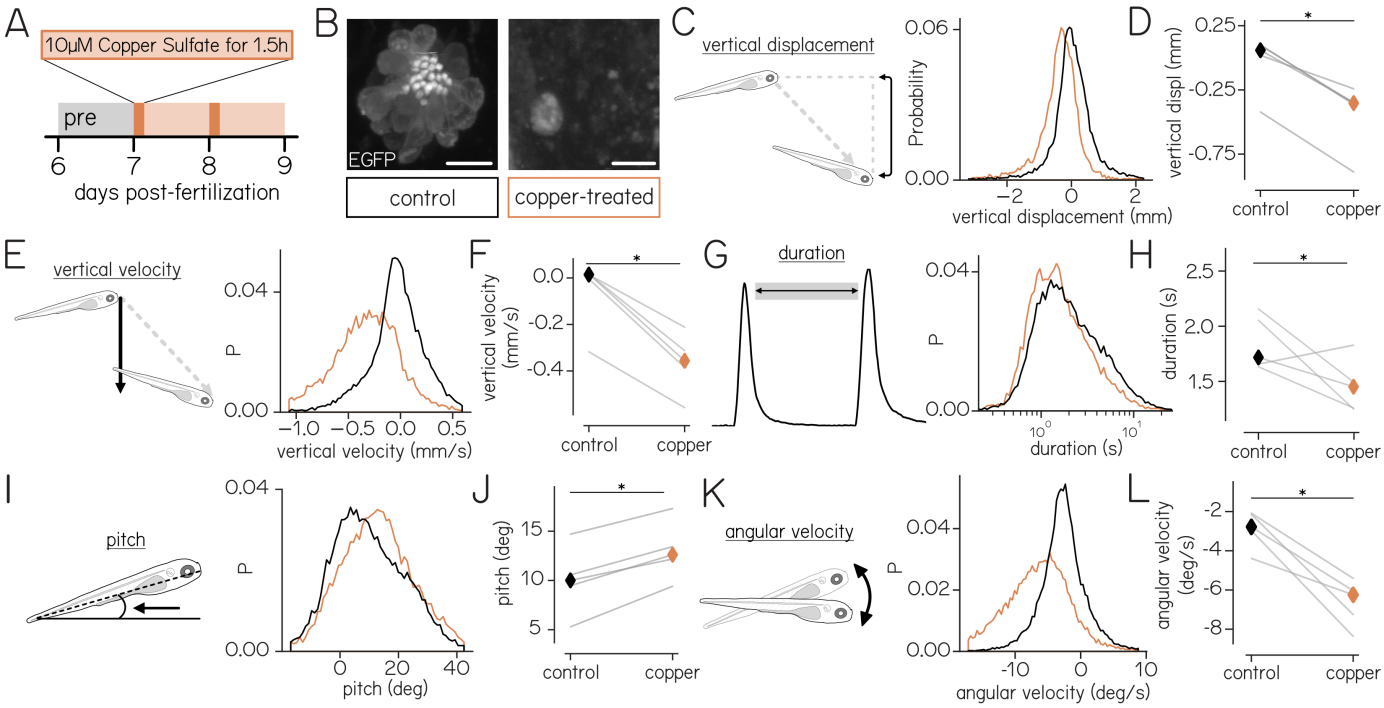

Figure 2: Copper treatment ablates lateral line hair cells and disrupts stability.
(A) Experimental timeline indicating pre-treatment recording (grey), treatment periods (dark orange), and post-treatment recording (light orange). Full sample numbers and statistics in Table 2.
(B) Confocal images of a control (left) and a copper-treated (right) SO2 neuromast transgenically labelled with EGFP in 7 dpf larvae. Complete loss of hair cells follows copper treatment. Scale bar = 10μm.
(C) Schematic (left) and distribution (right) of vertical displacement between bouts. Orange are copper-treated larvae, black untreated siblings.
(D) Median displacement in depth during the inter-bout interval is significantly lower in copper-treated larvae (p=0.0219). Grey lines connect treatment conditions for experimental repeats (siblings).
(E) Schematic and distributions of vertical velocity during the inter-bout interval.
(F) Median vertical velocity is lower (i.e. downward) in copper-treated larvae (p=0.00928).
(G) Schematic (left) and distribution (right) of inter-bout interval duration.
(H) Median inter-bout interval duration is lower for copper-treated larvae (p=0.03405).
(I) Schematic (left) and distribution (right) of inter-bout interval pitch.
(J) Median inter-bout interval pitch is higher in copper-treated larvae (p=0.001).
(K) Schematic (left) and distribution (right) of angular velocity during the inter-bout interval.
(L) Median inter-bout interval angular velocity is lower (i.e. nose-down rotation) in copper-treated larvae. (p=4.6e-4).
P, probability.

The sinking and increased angular velocity are similar to — but considerably milder than — behaviors observed in larvae that inflate their swim bladders with oil instead of air [11,19]. There, larvae compensate for their increased density, maintaining elevation by (1)

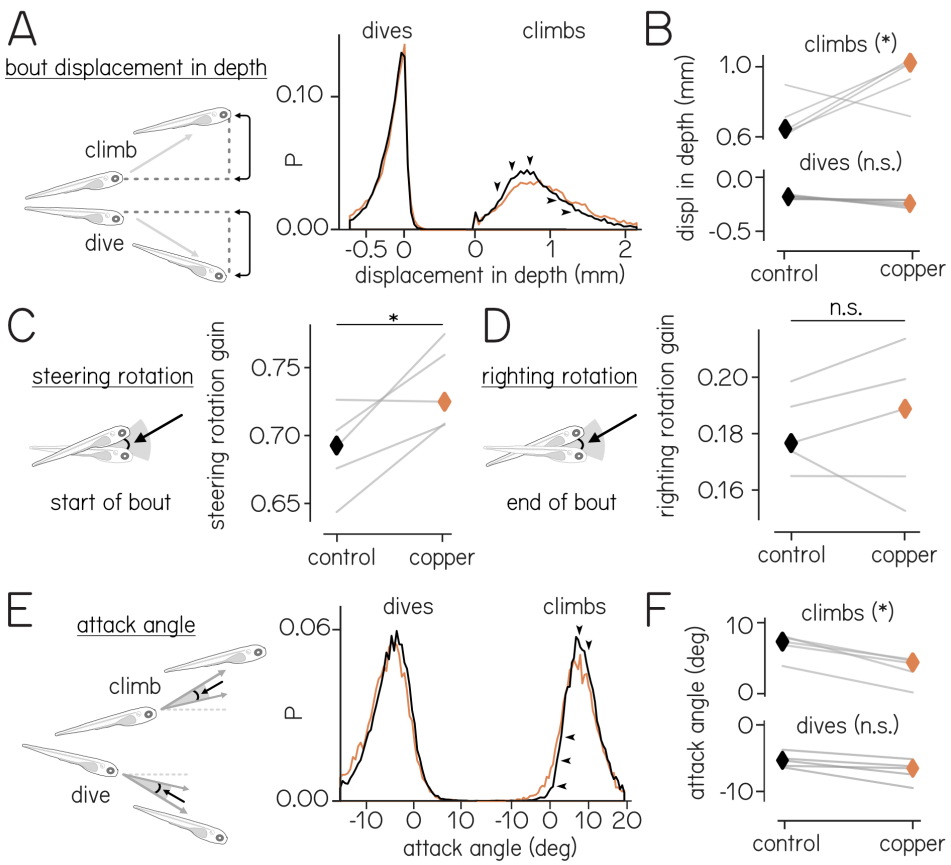

Figure 3: Copper-treated larvae rely on trunk rotations to produce climb bouts with greater vertical displacement.
(A) Schematic (left) and distribution (right) of displacement in depth during climbing and diving bouts.
(B) Median displacement in depth is greater in copper-treated larvae for climbs (top; p=0.01468) but not dives (bottom; p=0.0807).
(C) Steering rotation gain is higher in copper-treated larvae (p=0.04204).
(D) Righting rotation gain does not change between treatment groups (p=0.81049).
(E) Schematic (left) and distribution (right) of attack angle during climbing and diving bouts.
(F) Median attack angle is less in copper-treated larvae for climbs (top; p=0.01707) but not dives (bottom; p=0.13825).
See Table 2 for full statistics and Table 6 for breakdown of bouts. Unpaired t-test. P, probability; NS, not significant.

swimming more frequently to correct destabilizing nose-down torques, and (2) adopting a more nose-up posture to add an upward component to each bout. When observed, copper-treated larvae moved more frequently and maintained a more nose-up posture. We infer that lateral line loss leads larvae to change postural behavior, most likely due to changes to buoyancy.

Larvae compensate for instability by engaging trunk rotations to climb

To investigate how lateral line loss might influence kinematics, we examined the statistics of swim bouts after copper treatment. Swim speed was comparable between treatment conditions (copper: 15.03 [10.19] mm/s vs. control: 11.45 [6.67] mm/s, p=0.09274). The average bout trajectory was also similar (copper: 12.46 [26.46]° vs. 9.64 [29.06]°, p=0.31979). We separated bouts with an upward trajectory (climbs) from those with a downward trajectory (dives, Figure 3A), since only climbs would countermand sinking associated with copper treatment. When climbing, copper-treated larvae moved significantly higher in depth compared to controls (0.96 [0.81] mm vs. 0.68 [0.56] mm, p=0.01468, Figure 3B). In contrast, depth change was similar during dives (copper: -0.20 [0.34] mm, vs. control: -0.16 [0.24] mm, p=0.0807; Figure 3B). We conclude that while copper-treated larvae swam comparably to untreated siblings, their climbs produced greater increases in elevation.

During bouts, larvae perform two different angular rotations with different purposes: they rotate their trunks to change trajectory in the accelerative phase (steering), and rotate in the decelerative phase to restore posture (righting). The strength of these behaviors can be parameterized as the steering and righting gains, as these metrics reflect foundational kinematic features of swim bouts in the vertical axis [12,19]. To estimate the degree to which bout trajectory relied on trunk rotations, we investigated the gain of the steering and righting rotations. Steering gain is defined as the slope of the best-fit line between posture and trajectory evaluated at the time of peak speed [12]. If the trajectory of a given bout can be explained by the posture at the time of peak speed, the steering gain would be 1. Steering gain of copper-treated larvae was greater than untreated siblings (0.72 vs. 0.69, p=0.04204, Figure 3C). The gain of the righting rotation is defined as the slope of the best-fit line between posture at the beginning of the bout and posture change from peak speed to 100 ms after peak speed. If the rotation completely restored posture, the gain would be 1. The righting rotation gain did not differ between copper-treated and sibling larvae (0.19 vs. 0.18, p=0.81049, Figure 3D).

Larval zebrafish use a second effector, their pectoral fins, to generate lift when climbing [12,14]. Fin-related lift can be dissociated from steering-related changes by measuring the difference between the predicted trajectory based on posture and the observed trajectory ("attack angle," Figure 3E). Attack angles are largely abolished by acute loss of the pectoral fins [12,14]. As expected, attack angles were positive for climbs and negative for dives, regardless of treatment group. Copper-treated larvae generated less lift, seen as lower attack angles during climbs than sibling controls (3.82 [5.08]° vs. 6.95 [5.88]°; p=0.01707, Figure 3F). However, dive bout attack angles were comparable between groups (control: -5.14 [5.40]°; copper: -6.18 [6.18]°; p=0.13825). We infer that in the dark, copper-treated larvae relied more on trunk rotations than fin-generated lift to climb.

Taken together, we conclude that in the dark, the main way larvae restore posture is by selectively increasing their trunk rotations to climb more. Greater elevation during climbs would counteract passive sinking that follows loss of lateral line hair cells.

Vision changes compensatory strategies after lateral line hair cell ablation

We hypothesized that visual input would change postural control strategies after lateral line hair cell loss. To define the consequences of visual feedback, we repeated our experiments in a standard 14/10 light/dark cycle, instead of in the dark (Figure 4A). All comparisons used data gathered during circadian day (Tables 2 and 4). As expected [22], both copper-treated and untreated larvae moved more

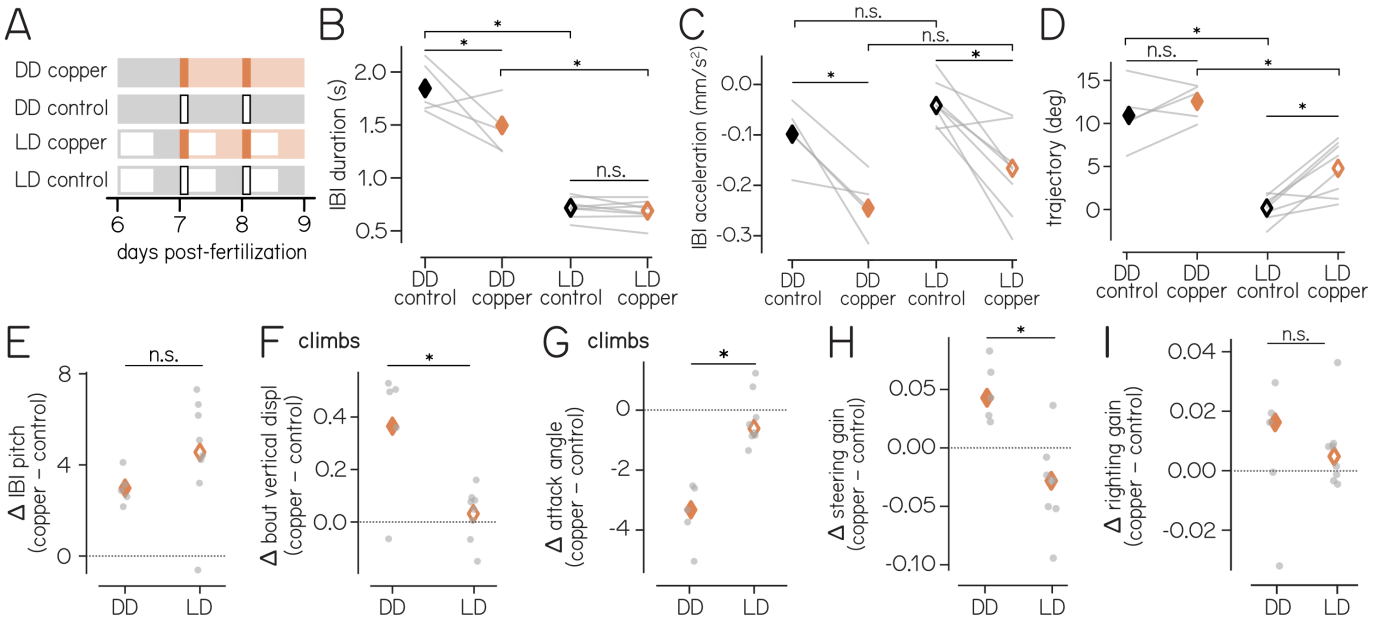

Figure 4: Copper-treated larvae are similarly unstable and adopt different posture and kinematic strategies in the light and in the dark
(A) Experimental timeline of each lighting condition (filled = dark, open = light) and treatment (grey = control, orange = copper). Treatment times indicated in dark orange. Full sample numbers and statistics in Table 4 and bout breakdown in Table 6.
(B) Inter-bout interval (IBI) durations are higher in the dark than in the light (control : p=0.001, copper: p=0.001). Copper-treatment shortens IBI duration in the dark (p=0.0063) but not the light (p=0.900).
(C) Vertical acceleration during the IBI is lower (more downward) in copper-treated larvae in both the dark (p=0.0099) and the light (p=0.0017). Acceleration did not vary as a function of light for control (p=0.3602) or copper-treated larvae (p=0.2898).
(D) Median swim trajectory of copper-treated larvae is higher than untreated siblings in the light (p=0.017) but not the dark (p=0.5466). Trajectories are lower (more horizontal) in the light (control: p=0.001, copper: p=0.001).
(E–I) Data are plotted as the difference between control and copper-treated larvae for each experimental repeat (gray circles) for both lighting conditions. Dotted lines at 0 indicate no difference between copper-treated and untreated siblings. p-values are comparisons of the differences in the dark vs. light.
(E) Differences in IBI pitch are similar between dark and light (p=0.20163).
(F) Differences in vertical displacement during climb bouts are minute in the light, unlike the dark (p=0.02243).
(G) Differences in attack angle for climb bouts are small in the light, unlike the dark (p=0.00011).
(H) Differences in steering rotation gain are higher in the dark and lower in the light (p=0.00174).
(I) Differences in righting rotation gain are unchanged (p=0.98070) .
Multiple comparison test for panels B–D (all p-values listed in Table 4). Unpaired t-test for panels E–I. DD, dark-dark; LD, light-dark; IBI, inter-bout interval; NS, not significant; P, probability.

frequently in the light (Figure 4B). The inter-bout interval duration in the light was shorter for both treatment conditions (copper LD: 0.65 [0.50] s vs. DD: 1.45 [1.52] s, p=0.001 — untreated LD: 0.70 [0.55] s vs. DD: 1.78 [2.27] s, p=0.001). We saw no difference in movement frequency in the light between copper-treated and untreated siblings (1.54 [2.0] s^{-1} vs. 1.42 [1.82] s^{-1}, p=0.9). However, we observed fewer overall bouts in copper-treated fish than controls in the light (n=118404 vs n=173386).

We next asked if the physical challenges faced by copper-treated larvae were comparable in the light and the dark. To do so in a way that would be independent of duration, we compared linear acceleration during the inter-bout interval. Instability was comparable in both the light and dark during the inter-bout interval. Copper-treated larvae showed more acceleration in the downward direction than untreated siblings in both the light and the dark (DD copper: -0.24 [0.76] mm/s^2 vs. DD untreated: -0.09 [0.44] mm/s^2, p=0.0099; LD copper: -0.17 [0.88] mm/s^2 vs. LD untreated -0.03 [0.67] mm/s^2, p=0.0017, Figure 4C). Crucially, downward acceleration did not change between light and dark for (copper LD vs. DD: p=0.2898, untreated LD vs. DD: p=0.3602). As linear acceleration was comparable in both light and dark regardless of treatment, we conclude that the changes after copper treatment reflect changes to buoyancy.

Given the comparable physical challenges to maintaining elevation, we next asked if compensatory strategies were similar after copper-treatment in the light and dark (Table 4). Unlike in the dark, copper-treated larvae in the light climbed more frequently than untreated siblings (copper trajectory: 4.03 [21.39]° vs. untreated trajectory: -1.48 [17.85]°, p=0.017, Figure 4D). However, similar to copper-treated larvae in the dark, those in the light adopted a more nose-up posture than untreated siblings (4.86 [16.50]°vs. -0.43 [14.65]°, p=0.0045). In the light, copper-treated larvae relied less on trunk steering to climb, instead engaging their fins to produce lift. When climbing in the light, copper-treated and untreated siblings produced comparable displacements in depth (LD control: 0.19 [0.24] mm, vs. LD copper: 0.21 [0.28] mm, p=0.09109). Attack angles (fin engagement) were also comparable between copper-treated and untreated siblings in the light (LD control: 1.87 [4.07]°, vs. LD copper: 1.63 [4.49]°, p=0.45536). In the light, steering gain (trunk use) was unchanged between copper-treated larvae than untreated siblings (LD control: 0.76 vs. LD copper: 0.72 , p=0.09151), as was righting gain (LD control: 0.09 vs. LD copper: 0.10, p=0.25570). Compared to dark recordings, copper-treated larvae in the light changed their strategy for climbing, as shown by less reliance on climbing displacements (Figure 4F), lift from pectoral fins (Figure 4G), and body rotations (Figure 4H), while maintaining similar changes to inter-bout interval posture (Figure 4E) and postural corrections during bouts (Figure 4I).

Taken together, copper-treated larvae in the light experience comparable destabilization but regulate their climbs differently. We conclude that visual feedback changes the strategy that larvae use to control posture and trajectory for elevation restoration after lateral line hair cell loss.

DISCUSSION

Here we defined the postural and kinematic responses that follow imposed instability (decreased buoyancy) in both the light and dark. We exposed larvae to a copper treatment that killed the hair cells of the lateral line. This manipulation produced larvae that appeared less buoyant, sinking and rotating nose-down more severely between swim bouts. These larvae changed the way they swam, and the nature of these changes varied depending on whether larvae were in the dark or the light. In the dark, larvae without lateral line hair cells swam more frequently, and when they climbed, they relied on trunk rotations to climb more effectively. Conversely, in the light, larvae without hair cells changed their trajectories to climb more often, and did so with a combination of fin lift and trunk rotation. Our results argue that larvae can sense changes in body density, adjust their behavior to compensate, and switch compensatory strategies when visual feedback is available. We propose that larval zebrafish attempt to regulate elevation by controlling posture. As neural circuits for multisensory control of posture are evolutionarily conserved, our findings set the stage to explore how vertebrates represent and maintain their position in space.

The lateral line, the swim bladder, and buoyancy

Classical work has defined the role of the lateral line[3], while recent studies have expanded our understanding of this remarkable organ. Functional investigation of the lateral line has demonstrated sophisticated comparisons of expected and observed patterns of flow during swimming[23–27]. Studies of lateral line neuromasts have revealed foundational principles of patterning[28,29], organogenesis[30,31], molecular and functional descriptions of hair cells[32–34], and sensitivity to ototoxic compounds[35,36]. Advances in machine vision enable long duration recordings of freely swimming larvae, which implicate the lateral line in natural behaviors such as social avoidance[37] and excitingly, spatial dispersal[38]. We propose that, by taking steps towards understanding the postural consequences of lateral line loss, our work here similarly broadens our view.

After copper exposure, larvae in both the light and dark sink as if they are less buoyant. We do not know precisely how loss of lateral line hair cells affects density. The mass of both the copper sulfate and lost hair cells is negligible, such that we do not think that this is a direct effect of treatment. Hair cell death occurs by different signaling pathways, even within a specific pharmacological category such as aminoglycoside antibiotics[39]. Different ototoxic compounds (neomycin and copper sulfate) produce different effects on rheotaxis[21], though this may reflect non-specific effects of neomycin on muscle tissue[20]. While long-term copper exposure can be neurotoxic[40–42], such toxicity has not been demonstrated for the short exposures used in our study and other recent work[38]. We therefore do not believe non-specific toxicity is likely to be a major confound. Future studies could use complementary ototoxic agents such as gentamicin to investigate the specificity of copper-mediated changes.

Zebrafish, like other teleosts, achieve near-neutral buoyancy by inflating a gas-filled organ called the swim bladder[17,43]. The ability of the autonomic nervous system to regulate swim bladder volume[44] emerges at the juvenile state[45]. Larval zebrafish must instead gulp air at the water's surface to inflate the swim bladder[15], maintaining volume by control of a sphincter at the junction of the pneumatic duct of the swim bladder and the esophagus[16]. Constitutive and early loss of the head neuromasts of the anterior lateral line[46,47] leads ~50% of larval zebrafish to over-inflate their swim bladders by gulping more air at the surface[38,48]. We propose that our copper treatment similarly affects the esophageal sphincter, leading to a transient secretion of gas that decreases the volume of the swim bladder. While determining the exact mechanism by which copper treatment leads to a decrease in buoyancy is beyond the scope of this manuscript, our work nonetheless supports the relationship between the lateral line, the swim bladder, and buoyancy. Future work examining the transmission of information from the anterior lateral line afferents to cranial nerves that regulate the esophagus will establish the circuit responsible for buoyancy and allow insight into the functional consequences of copper exposure.

Multisensory strategies to regulate elevation

Discovering that copper-treated zebrafish appear less buoyant allowed us to investigate how larvae attempt to regulate elevation. Previously, we had proposed that larvae maintain a slightly nose-up posture to ensure that in-plane forward translations, which comprise most swim bouts, would contain an upward component that allowed them to maintain elevation[11,19]. Increasing density by raising larvae with oil-inflated swim bladders led larvae to swim with upward trajectories, while decreasing density by letting larvae swim in 1.5% glycerol led larvae to swim with downward trajectories[11,19]. Unlike non-specific health concerns related to oil and glycerol, transient copper treatment was compatible with long-term behavioral monitoring. Consequentially, we could characterize strategies larvae adopt when buoyancy is challenged.

The multisensory nature of elevation control is apparent when considering whether the behavioral changes we see are effective. We observed many fewer bouts after copper treatment: 40% of total control bouts in the dark, and 68% in the light (Table 6). SAMPL only images the middle of the behavioral arena, and caution is warranted when making inferences about things we cannot see. However, the reduced number of bouts and the downward accelerations suggest that copper-treated larvae likely sit at the bottom of the arena. We therefore propose that the decrease in bouts observed are due to ineffective control of elevation. Why then do larvae not simply swim to the surface and re-inflate their swim bladders, or adopt even more eccentric postures, as they do when their swim bladders are full of oil? Intriguingly, recent work with a slightly different $CuSO_4$ protocol suggests that different conditions (e.g., dose, timing, recovery) can lead fish to the opposite effect: overinflation and increased buoyancy[38]. We suggest that proper control of buoyancy and elevation requires a functional lateral line, as vestibular signals—either alone or together with visual feedback—are insufficient for normal behavior. Such multisensory integration is consistent with other reports of visually-mediated changes to lateral line-dependent behavior[49,50].

Our finding that strategies for elevation control reflect multisensory integration supports a neuronal origin for our behavioral observations. One possible substrate for the convergence of visual, vestibular, and potentially lateral line information is a midbrain nucleus comprised of spinal-projecting neurons called the interstitial nucleus of Cajal, a.k.a. the nucleus of the medial longitudinal fasciculus (INC/nucMLF)[13,51–55]. The INC/nucMLF receives projections from ascending vestibular neurons in the tangential nucleus[13,54,56,57]. Alternatively, both tectal[58] and vestibulo-spinal neurons[59–61] receive sensory input from a wide variety of modalities[62] and may be involved in relevant computations. Lastly, the cerebellum integrates vestibular[63–66], visual[67,68], and lateral line inputs[69,70], and controls posture in larval zebrafish[71]. Cerebellar input originates in part in the inferior olive, which has recently been shown to play a role in positional homeostasis in the yaw axis[72]. Recent advances in functional imaging of neuronal activity during presentation of flow and body tilts[54,60,72–75] together with connectomic characterization of neuronal projections[76] offer the promise of understanding integration of vestibular-, visual-, and lateral line-derived signals for control of posture and elevation.

Conclusion

Regulation of elevation is vital for aquatic vertebrates[6,7]. We discovered that larvae sank after acute loss of the lateral line. Consequentially, they changed both posture and swimming kinematics. However, changes to control strategies and effectors (i.e., trunk and fins)

varied when visual feedback was available. Our work reveals the multisensory nature of the computations that enable larval zebrafish to maintain their position in depth, framing future investigation into how the vertebrate brain represents and controls elevation.

MATERIALS AND METHODS

Animals

All procedures involving larval zebrafish (*Danio rerio*) were approved by the New York University Langone Health Institutional Animal Care & Use Committee (IACUC). Zebrafish larvae were raised at 28.5°C on a standard 14/10 h light/dark cycle at a density of 20–50 larvae in 25-40 ml of E3 medium before 5 days post-fertilization (dpf). During experiments (6–8 dpf) larvae were fed cultured rotifers (Reed Mariculture) for 30 minutes.

Zebrafish lines

Behavioral experiments were performed on the Schoppik lab's wild-type background (AB/WIK/TU mix, characterized originally for SAMPL [12]). Imaging experiments used the *Tg(myo6b:actb1-EGFP)* transgenic line to label lateral line hair cells.

Behavior and Copper Treatment

Freely moving larvae were measured using the extensively described SAMPL method [12]. In brief, 6–8 larvae were placed into custom vertical chambers (25mL volume, 50mm x 50mm x 10mm) filled with E3. Chambers were placed between an infrared light source (940nm) and a camera fit with an infrared filter (Edmund Optics). Recordings were performed in a light-tight enclosure with optional light control inside the box. The field of view (400 mm^2) was sampled from the lower middle of the chamber at a rate of 166 frames per second.

Experiments began at 6 days post-fertilization (dpf) with 24 hours of recording. Larvae were then treated with 10 µM copper sulfate ($CuSO_4$; Acros Organics 197722500) in E3 or untreated (transferred to E3 alone) for 90 minutes. Untreated fish were transferred and handled identically to copper-treated larvae. Larvae were then returned into chambers for 24 hours of post-treatment recording. Copper sulfate treatment was repeated after 24 hours to avoid hair cell regeneration [77]. A total of 5 experimental repeats using sibling controls were completed in the dark (n=114 larvae per condition), and 8 in the light (n=150 larvae per condition).

Extensive description of SAMPL analyses and a full Python-based analysis suite is freely available [12]. Briefly, swim bouts were extracted from captured epochs and aligned to peak speed, defined as 0 ms. Bouts were defined from -250 ms to +200 ms relative to peak speed. Bout trajectories were classified by the angle of trajectory at peak speed; control data for each lighting condition was divided into thirds to determine bin edges so that a third of the dataset fell into each navigational category (climb, flat, and dive). The same bin edges were applied to copper-treated larvae for the respective lighting condition and control dataset.

Imaging

One hour after copper treatment, larvae were followed by three 5-minute washes with E3. Larvae were next anesthetized in MESAB (Sigma-Aldrich E10521) until they were non-responsive to tap stimuli, then dorsally mounted in 2% low- melting point agarose in E3 for imaging. The SO2 neuromast was identified on control and copper-treated larvae using a confocal microscope (Zeiss LSM800) equipped with a 20x water-immersion objective (1.0 NA). All images were analyzed using Fiji/ImageJ [78].

Statistical Analysis

Sample sizes were determined using extensive characterization of wild-type variability [12]. Results are reported as median [interquartile range] as raw data were not normally distributed. Significance was set at $\alpha = 0.05$. When experimental repeats were normally distributed, comparisons used unpaired t-tests; nonparametric data comparisons were performed with Wilcoxon rank-sum tests. Effect size was estimated for normally distributed data using Cohen's d [79]. Steering and righting gain was calculated using values from each experimental repeat, and is reported of the median of repeats.

Data sharing

All raw data and code for analysis are available at the Open Science Framework DOI 10.17605/OSF.IO/BWM2E

ACKNOWLEDGMENTS

Research was supported by the National Institute on Deafness and Communication Disorders of the National Institutes of Health under award numbers R01DC017489, the National Institute of Neurological Disorders and Stroke under award number R61NS125280, by the Leon Levy Foundation (YZ), the Rainwater Charitable Foundation (YZ) and by the Irma T. Hirschl/Monique Weill-Caulier Trust (DS). The authors would like to thank Hannah Gelnaw for assistance with fish care, Lavinia Sheets and lab for sharing the *Tg(myo6b:actb1-EGFP)* line, and the members of the Schoppik and Nagel labs for their valuable feedback and discussions.

AUTHOR CONTRIBUTIONS

Conceptualization: YZ; Methodology: YZ; Investigation: SD, YZ; Visualization: SD; Writing: DS, SD; Editing: SD, DS; Funding Acquisition: DS, YZ; Supervision: DS.

AUTHOR COMPETING INTERESTS

The authors have no competing interests to declare.

REFERENCES

1. Jay M. Goldberg, Victor J. Wilson, Kathleen E. Cullen, Dora E. Angelaki, Dianne M. Broussard, Jean A. Büttner-Ennever, Kikuro Fukushima, and Lloyd B. Minor. *The Vestibular System in Everyday Life*, page 220. Oxford University Press, March 2012.
2. John C. Tuthill and Eiman Azim. Proprioception. *Current Biology*, 28(5):R194R203, March 2018.
3. S. Dijkgraaf. The functioning and significance of the lateralline organs. *Biological Reviews*, 38(1):51105, February 1963.
4. Yuri Glebovich Aleyev. *Nekton*. Dr. W. Junk, 1977.
5. P. W. Webb. Control of posture, depth, and swimming trajectories of fishes. *Integrative and Comparative Biology*, 42(1):94–101, 2002.
6. R. M. Alexander. Physical aspects of swimbladder function. *Biological Reviews*, 41(1):141176, February 1966.
7. B. Pelster. *Buoyancy Control in Aquatic Vertebrates*, page 6598. Springer Berlin Heidelberg, 2009.
8. CD Wilga and GV Lauder. Function of the heterocercal tail in sharks: quantitative wake dynamics during steady horizontal swimming and vertical maneuvering. *Journal of Experimental Biology*, 205(16):2365–2374, 2002.
9. Martha W Bagnall and David Schoppik. Development of vestibular behaviors in zebrafish. *Current Opinion in Neurobiology*, 53:83–89, 2018.
10. João C. Marques, Simone Lackner, Rita Félix, and Michael B. Orger. Structure of the zebrafish locomotor repertoire revealed with unsupervised behavioral clustering. *Current Biology*, 28(2):181–195.e5, 2018.
11. David E. Ehrlich and David Schoppik. Control of movement initiation underlies the development of balance. *Current Biology*, 27(3):334344, February 2017.

12. Yunlu Zhu, Franziska Auer, Hannah Gelnaw, Samantha N. Davis, Kyla R. Hamling, Christina E. May, Hassan Ahamed, Niels Ringstad, Katherine I. Nagel, and David Schoppik. Sampl is a high-throughput solution to study unconstrained vertical behavior in small animals. *Cell Reports*, 42(6):112573, June 2023.
13. Takumi Sugioka, Masashi Tanimoto, and Shin ichi Higashijima. Biomechanics and neural circuits for vestibular-induced fine postural control in larval zebrafish. *Nature Communications*, 14(1), March 2023.
14. David E Ehrlich and David Schoppik. A primal role for the vestibular sense in the development of coordinated locomotion. *eLife*, 8, October 2019.
15. E. M. Goolish and K. Okutake. Lack of gas bladder inflation by the larvae of zebrafish in the absence of an airwater interface. *Journal of Fish Biology*, 55(5):10541063, November 1999.
16. Jessica L. Finney, George N. Robertson, Chantelle A.S. McGee, Frank M. Smith, and Roger P. Croll. Structure and autonomic innervation of the swim bladder in the zebrafish (danio rerio). *The Journal of Comparative Neurology*, 495(5):587606, 2006.
17. William J. Stewart and Matthew J. McHenry. Sensing the strike of a predator fish depends on the specific gravity of a prey fish. *Journal of Experimental Biology*, 213(22):37693777, November 2010.
18. Matthew J. McHenry and George V. Lauder. The mechanical scaling of coasting in zebrafish (danio rerio). *Journal of Experimental Biology*, 208(12):22892301, June 2005.
19. David E. Ehrlich and David Schoppik. A novel mechanism for volitional locomotion in larval zebrafish. *bioRxiv*, September 2017.
20. Eunjung Han, Kyoung Ho Oh, Saemi Park, Yoon Chan Rah, Hae-Chul Park, Soonil Koun, and June Choi. Analysis of behavioral changes in zebrafish (danio rerio) larvae caused by aminoglycoside-induced damage to the lateral line and muscles. *NeuroToxicology*, 78:134–142, May 2020.
21. Kyle C. Newton, Dovi Kacev, Simon R. O. Nilsson, Allison L. Saettele, Sam A. Golden, and Lavinia Sheets. Lateral line ablation by ototoxic compounds results in distinct rheotaxis profiles in larval zebrafish. *Communications Biology*, 6(1), January 2023.
22. David A. Prober, Jason Rihel, Anthony A. Onah, Rou-Jia Sung, and Alexander F. Schier. Hypocretin/orexin overexpression induces an insomnia-like phenotype in zebrafish. *The Journal of Neuroscience*, 26(51):1340013410, December 2006.
23. Elias T. Lunsford, Dimitri A. Skandalis, and James C. Liao. Efferent modulation of spontaneous lateral line activity during and after zebrafish motor commands. *Journal of Neurophysiology*, 122(6):24382448, December 2019.
24. Gema Valera, Daniil A. Markov, Kayvan Bijari, Owen Randlett, Amir Asgharsharghi, Jean-Pierre Baudoin, Giorgio A. Ascoli, Ruben Portugues, and Hernán López-Schier. A neuronal blueprint for directional mechanosensation in larval zebrafish. *Current Biology*, 31(7):1463–1475.e6, April 2021.
25. Paul Pichler and Leon Lagnado. Motor behavior selectively inhibits hair cells activated by forward motion in the lateral line of zebrafish. *Current Biology*, 30(1):150–157.e3, January 2020.
26. Dimitri A. Skandalis, Elias T. Lunsford, and James C. Liao. Corollary discharge enables proprioception from lateral line sensory feedback. *PLOS Biology*, 19(10):e3001420, October 2021.
27. Iris Odstrcil, Mariela D. Petkova, Martin Haesemeyer, Jonathan Boulanger-Weill, Maxim Nikitchenko, James A. Gagnon, Pablo Oteiza, Richard Schalek, Adi Peleg, Ruben Portugues, Jeff W. Lichtman, and Florian Engert. Functional and ultrastructural analysis of reafferent mechanosensation in larval zebrafish. *Current Biology*, 32(1):176–189.e5, January 2022.
28. Joaquin Navajas Acedo, Matthew G. Voas, Richard Alexander, Thomas Woolley, Jay R. Unruh, Hua Li, Cecilia Moens, and Tatjana Piotrowski. Pcp and wnt pathway components act in parallel during zebrafish mechanosensory hair cell orientation. *Nature Communications*, 10(1), September 2019.
29. Adrian Jacobo, Agnik Dasgupta, Anna Erzberger, Kimberly Siletti, and A.J. Hudspeth. Notch-mediated determination of hair-bundle polarity in mechanosensory hair cells of the zebrafish lateral line. *Current Biology*, 29(21):3579–3587.e7, November 2019.
30. Weiyi Qian, Naoya Yamaguchi, Patrycja Lis, Michael Cammer, and Holger Knaut. Pulses of rhoa signaling stimulate actin polymerization and flow in protrusions to drive collective cell migration. *Current Biology*, December 2023.
31. Hannah M. Olson, Amanda Maxfield, Nicholas L. Calistri, Laura M. Heiser, Weiyi Qian, Holger Knaut, and Alex V. Nechiporuk. Rhoa gef mcf2lb regulates rosette integrity during collective cell migration. *Development*, 151(1), January 2024.
32. Tuo Shi, Marielle O Beaulieu, Lauren M Saunders, Peter Fabian, Cole Trapnell, Neil Segil, J Gage Crump, and David W Raible. Single-cell transcriptomic profiling of the zebrafish inner ear reveals molecularly distinct hair cell and supporting cell subtypes. *eLife*, 12, January 2023.
33. Elias T. Lunsford, Yuriy V. Bobkov, Brandon C. Ray, James C. Liao, and James A. Strother. Anion efflux mediates transduction in the hair cells of the zebrafish lateral line. *Proceedings of the National Academy of Sciences*, 120(52), December 2023.
34. Hiu-Tung C. Wong, Daria Lukasz, Catherine M. Drerup, and Katie S. Kindt. In vivo investigation of mitochondria in lateral line afferent neurons and hair cells. *Hearing Research*, 431:108740, April 2023.
35. Allison B. Coffin, Emily Dale, Emilee Doppenberg, Forrest Fearington, Tamasen Hayward, Jordan Hill, and Olivia Molano. Putative covid-19 therapies imatinib, lopinavir, ritonavir, and ivermectin cause hair cell damage: A targeted screen in the zebrafish lateral line. *Frontiers in Cellular Neuroscience*, 16, August 2022.
36. Samantha N. Davis, Patricia Wu, Esra D. Camci, Julian A. Simon, Edwin W. Rubel, and David W. Raible. Chloroquine kills hair cells in zebrafish lateral line and murine cochlear cultures: Implications for ototoxicity. *Hearing Research*, 395:108019, September 2020.
37. Antonia H. Groneberg, João C. Marques, A. Lucas Martins, Ruth Diez del Corral, Gonzalo G. de Polavieja, and Michael B. Orger. Early-life social experience shapes social avoidance reactions in larval zebrafish. *Current Biology*, 30(20):4009–4021.e4, October 2020.
38. Allia Lin, Efrén Álvarez Salvado, Nikola Milicic, Nimish Pujara, and David E. Ehrlich. Multisensory navigational strategies of hatchling fish for dispersal. *Current Biology*, 33(22):4917–4925.e4, November 2023.
39. Allison B. Coffin, Edwin W. Rubel, and David W. Raible. Bax, bcl2, and p53 differentially regulate neomycin- and gentamicin-induced hair cell death in the zebrafish lateral line. *Journal of the Association for Research in Otolaryngology*, 14(5):645–659, July 2013.
40. Felix Bulcke, Ralf Dringen, and Ivo Florin Scheiber. *Neurotoxicity of Copper*, page 313343. Springer International Publishing, 2017.
41. Yuhao Li, Yan Sun, Gong Zhang, Zizi He, Yajie Wang, and Jianlin Cui. Effects of copper oxide nanoparticles on developing zebrafish embryos and larvae. *International Journal of Nanomedicine*, page 905, March 2016.
42. Siying Chen, Yingju Qin, Xiaolin Ye, Jian Liu, Xiliang Yan, Li Zhou, Xiaohong Wang, Christopher J. Martyniuk, and Bing Yan. Neurotoxicity of the cu(oh)2 nanopesticide through perturbing multiple neurotransmitter pathways in developing zebrafish. *Environmental Science & Technology*, 57(48):1940719418, November 2023.
43. Benjamin W. Lindsey, Frank M. Smith, and Roger P. Croll. From inflation to flotation: Contribution of the swimbladder to whole-body density and swimming depth during development of the zebrafish (danio rerio). *Zebrafish*, 7(1):8596, March 2010.
44. Frank M. Smith and Roger P. Croll. Autonomic control of the swimbladder. *Autonomic Neuroscience*, 165(1):140148, November 2011.
45. G.N. Robertson, C.A.S. McGee, T.C. Dumbarton, R.P. Croll, and F.M. Smith. Development of the swimbladder and its innervation in the zebrafish, danio rerio. *Journal of Morphology*, 268(11):967985, August 2007.
46. Miki Iwasaki, Hayato Yokoi, Tohru Suzuki, Koichi Kawakami, and Hironori Wada. Development of the anterior lateral line system through local tissuetissue interactions in the zebrafish head. *Developmental Dynamics*, 249(12):14401454, August 2020.
47. Nils Brehm, Nils Wenke, Keshia Glessner, and Melanie Haehnel-Taguchi. Physiological responses of mechanosensory systems in the head of larval zebrafish (danio rerio). *Frontiers in Robotics and AI*, 10, July 2023.
48. Alexandra Venuto, Stacey Thibodeau-Beganny, Josef G. Trapani, and Timothy Erickson. A sensation for inflation: initial swim bladder inflation in larval zebrafish is mediated by the mechanosensory lateral line. *Journal of Experimental Biology*, 226(11), June 2023.
49. Sheryl Coombs, Joe Bak-Coleman, and John Montgomery. Rheotaxis revisited: a multi-behavioral and multisensory perspective on how fish orient to flow. *Journal of Experimental Biology*, 223(23), December 2020.
50. Shayna-Lee Chaput, Warren W. Burggren, Peter L. Hurd, and Trevor J. Hamilton. Zebrafish (*Danio rerio*) shoaling in light and dark conditions involves a complex interplay between vision and lateral line. *Behavioural Brain Research*, 439:114228, February 2023.
51. Kristen E. Severi, Ruben Portugues, João C. Marques, Donald M. O'Malley, Michael B. Orger, and Florian Engert. Neural control and modulation of swimming speed in the larval zebrafish. *Neuron*, 83(3):692–707, August 2014.
52. Tod R. Thiele, Joseph C. Donovan, and Herwig Baier. Descending control of swim posture by a midbrain nucleus in zebrafish. *Neuron*, 83(3):679–691, August 2014.
53. Wei-Chun Wang and David L. McLean. Selective responses to tonic descending commands by temporal summation in a spinal motor pool. *Neuron*, 83(3):708–721, aug 2014.
54. Masashi Tanimoto, Ikuko Watakabe, and Shin ichi Higashijima. Tiltable objective microscope visualizes discrimination of static and dynamic head movement originates at hair cells. *Research Square*, July 2022.
55. Eva M. Berg, Leander Mrowka, Maria Bertuzzi, David Madrid, Laurence D. Picton, and Abdeljabbar El Manira. Brainstem circuits encoding start, speed, and duration of swimming in adult zebrafish. *Neuron*, 111(3):372–386.e4, February 2023.
56. Isaac H. Bianco, Leung-Hang Ma, David Schoppik, Drew N. Robson, Michael B. Orger, James C. Beck, Jennifer M. Li, Alexander F. Schier, Florian Engert, and Robert Baker. The tangential nucleus controls a gravito-inertial vestibulo-ocular reflex. *Current Biology*, 22(14):1285–1295, Jul 2012.
57. David Schoppik, Isaac H. Bianco, David A. Prober, Adam D. Douglass, Drew N. Robson, Jennifer M.B. Li, Joel S.F. Greenwood, Edward Soucy, Florian Engert, and Alexander F. Schier. Gaze-stabilizing central vestibular neurons project asymmetrically to extraocular motoneuron pools. *The Journal of Neuroscience*, 37(47):1135311365, September 2017.
58. Andrew W. Thompson, Gilles C. Vanwalleghem, Lucy A. Heap, and Ethan K. Scott. Functional profiles of visual-, auditory-, and water flow-responsive neurons in the zebrafish tectum. *Current Biology*, 26(6):743754, March 2016.
59. Zhikai Liu, Yukiko Kimura, Shin ichi Higashijima, David G.C. Hildebrand, Joshua L. Morgan, and Martha W. Bagnall. Central vestibular tuning arises from patterned convergence of otolith afferents. *Neuron*, 108(4):748–762.e4, November 2020.
60. Kyla R. Hamling, Yunlu Zhu, Franziska Auer, and David Schoppik. Tilt in place microscopy (TIPM): a simple, low-cost solution to image neural responses to body rotations. *The Journal of Neuroscience*, pages JN–RM–1736–22, December 2022.
61. Kyla R. Hamling, Katherine Harmon, and David Schoppik. The nature and origin of synaptic inputs to vestibulospinal neurons in the larval zebrafish. *eneuro*, 10(6):ENEURO.0090–23.2023, June 2023.
62. V. H. Sarkisian. Input-output relations of deiters' lateral vestibulospinal neurons with different structures of the brain. *Archives Italiennes de Biologie*, 138(4):295–353, 2000.
63. A. M. Pastor, R. R. de la Cruz, and R. Baker. Cerebellar role in adaptation of the goldfish vestibuloocular reflex. *Journal of Neurophysiology*, 72(3):13831394, September 1994.
64. S du Lac, J L Raymond, T J Sejnowski, and S G Lisberger. Learning and memory in the vestibulo-ocular reflex. *Annual Review of Neuroscience*, 18(1):409441, March 1995.

65. Timothy S Balmer and Laurence O Trussell. Selective targeting of unipolar brush cell subtypes by cerebellar mossy fibers. *eLife*, 8, April 2019.
66. Kathleen E. Cullen. Internal models of self-motion: neural computations by the vestibular cerebellum. *Trends in Neurosciences*, 46(11):9861002, November 2023.
67. Cristián Gutiérrez-Ibáñez, Douglas R. Wylie, and Douglas L. Altshuler. From the eye to the wing: neural circuits for transforming optic flow into motor output in avian flight. *Journal of Comparative Physiology A*, 209(5):839854, August 2023.
68. Koji Matsuda and Fumi Kubo. Circuit organization underlying optic flow processing in zebrafish. *Frontiers in Neural Circuits*, 15, July 2021.
69. Joachim Mogdans. The processing of hydrodynamic stimuli with the fish lateral line system, September 2022.
70. Matthew S. Weeg and Andrew H. Bass. Central lateral line pathways in a vocalizing fish. *The Journal of Comparative Neurology*, 418(1):4164, February 2000.
71. Franziska Auer, Katherine Nardone, Koji Matsuda, Masahiko Hibi, and David Schoppik. Purkinje cells control posture in larval zebrafish (*Danio rerio*). *bioRxiv*, September 2023.
72. En Yang, Maarten F. Zwart, Ben James, Mikail Rubinov, Ziqiang Wei, Sujatha Narayan, Nikita Vladimirov, Brett D. Mensh, James E. Fitzgerald, and Misha B. Ahrens. A brainstem integrator for self-location memory and positional homeostasis in zebrafish. *Cell*, 185(26):5011–5027.e20, December 2022.
73. Itia A. Favre-Bulle, Alexander B. Stilgoe, Halina Rubinsztein-Dunlop, and Ethan K. Scott. Optical trapping of otoliths drives vestibular behaviours in larval zebrafish. *Nature Communications*, 8(1), September 2017.
74. Gilles Vanwalleghem, Kevin Schuster, Michael A. Taylor, Itia A. Favre-Bulle, and Ethan K. Scott. Brain-wide mapping of water flow perception in zebrafish. *The Journal of Neuroscience*, 40(21):41304144, April 2020.
75. Natalia Beiza-Canelo, Hippolyte Moulle, Thomas Pujol, Thomas Panier, Geoffrey Migault, Guillaume Le Goc, Pierre Tapie, Nicolas Desprat, Hans Straka, Georges Debrégeas, and Volker Bormuth. Magnetic actuation of otoliths allows behavioral and brain-wide neuronal exploration of vestibulo-motor processing in larval zebrafish. *Current Biology*, 33(12):2438–2448.e6, June 2023.
76. Zhikai Liu, David G. C. Hildebrand, Joshua L. Morgan, Yizhen Jia, Nicholas Slimmon, and Martha W. Bagnall. Organization of the gravity-sensing system in zebrafish. *Nature Communications*, 13(1), August 2022.
77. Eric D. Thomas, Ivan A. Cruz, Dale W. Hailey, and David W. Raible. There and back again: development and regeneration of the zebrafish lateral line system. *WIREs Developmental Biology*, 4(1):116, October 2014.
78. Johannes Schindelin, Ignacio Arganda-Carreras, Erwin Frise, Verena Kaynig, Mark Longair, Tobias Pietzsch, Stephan Preibisch, Curtis Rueden, Stephan Saalfeld, Benjamin Schmid, Jean-Yves Tinevez, Daniel James White, Volker Hartenstein, Kevin Eliceiri, Pavel Tomancak, and Albert Cardona. Fiji: an open-source platform for biological-image analysis. *Nature Methods*, 9(7):676682, June 2012.
79. Jörn Lötsch and Alfred Ultsch. A non-parametric effect-size measure capturing changes in central tendency and data distribution shape. *PLOS ONE*, 15(9):e0239623, September 2020.

Table 1: Pre-treatment results for dark-dark dataset. Because the medians of each experimental repeats are normally distributed, p-values were calculated using unpaired t-tests (alpha = 0.05).

Parameter	Unit of Measure	Control Median	Control IQR	Copper Median	Copper IQR	P-Value
Inter-bout intervals						
Vertical displacement	mm	0.03	0.59	-0.01	0.66	0.73974
Vertical velocity	mm/s	-0.07	0.30	-0.11	0.39	0.54706
Duration	s	1.49	2.13	1.53	2.26	0.35909
Pitch	deg	14.34	20.61	15.65	18.86	0.62410
Angular velocity	deg/s	-2.71	3.69	-6.46	6.72	0.07000
Bouts						
Peak speed	mm/s	11.30	6.10	10.88	6.61	0.77783
Trajectory	deg	20.74	32.94	23.10	30.37	0.40075
Vertical displ (climb)	mm	0.90	0.62	0.93	0.65	0.42876
Vertical displ (dive)	mm	-0.09	0.26	-0.07	0.24	0.25141
Attack angle (climb)	deg	9.58	5.38	9.59	5.67	0.88099
Attack angle (dive)	deg	-3.87	5.97	-4.23	6.12	0.54215
Steering rotation gain		0.69		0.66		0.39809
Righting rotation gain		0.18		0.19		0.32206

Table 2: Effects of lateral line ablation in the dark Median ± IQR used for non-normal distributions of raw data. N = 114 control larvae, 114 copper-treated larvae. P-value calculated using unpaired t-test (alpha = 0.05) and effect size calculated using Cohen's D. Steering and righting rotation gain fit from 5 jackknife groups using all 45839 bouts (mean listed).

Parameter	Unit of Measure	n (bouts / IBI)	Control Median	Control IQR	Copper Median	Copper IQR	P-Value	Effect size	Significance
Inter-bout Interval									
Vertical displacement	mm	74028	0.021	0.62	-0.32	0.63	0.0219	-0.74	*
Vertical velocity	mm/s	74028	-0.02	0.29	-0.32	0.43	0.001	-1.19	*
Duration	s	74028	1.78	2.27	1.45	1.52	0.03405	-0.28	*
Pitch	deg	74028	8.65	17.64	12.42	16.82	0.00129	0.30	*
Angular velocity	deg/s	74028	-2.71	3.69	-6.46	6.73	4.6e-4	-1.06	*
Bout									
Peak speed	mm/s	45839	11.45	6.67	15.03	10.20	0.09274	0.63	
Trajectory	deg	45839	9.64	29.07	12.46	26.46	0.31979	0.13	
Vertical displacement (climb)	mm	15945	0.68	0.56	0.96	0.81	0.01468	0.59	*
Vetical displacement (dive)	mm	16788	-0.16	0.24	-0.20	0.34	0.0807	-0.22	
Attack angle (climb)	deg	15945	6.95	5.88	3.82	5.08	0.01707	-0.76	*
Attack angle (dive)	deg	16788	-5.14	5.40	-6.18	6.18	0.13825	-0.25	
Steering rotation gain			0.69		0.72		0.04204		*
Righting rotation gain			0.18		0.19		0.81049		

Table 3: IBI vertical velocity by time post-treatment. Early and late represent data collected in the first and second 5 hours after the treatment, respectively, for each 24-hour behavior session. Calculated using Dark-Dark dataset. P-value calculated using Wilcoxon rank sum (alpha = 0.05).

Treatment	Time Post-Treatment	Median	IQR	P-Value
Control	Early Late	-0.06 0.02	0.29 0.45	0.14164
Copper	Early Late	-0.3 -0.29	0.20 0.41	0.59081

Table 4: Effects of vision on swimming after lateral line loss Median ± IQR used for non-normal distributions of raw data. N = 150 LD control, 150 LD copper. P-value calculated using unpaired t-test (alpha = 0.05) and effect size calculated using Cohen's D.

Parameter	LD control median	LD control IQR	LD copper median	LD copper IQR	DD post control v. copper	LD post control v. copper	control DD v. LD	copper DD v. LD
Inter-bout interval								
Vertical displacement	-0.08	0.20	-0.09	0.22	0.00046	0.28555	0.54981	0.00409
Vertical velocity	-0.12	0.19	-0.21	0.28	0.001	0.2134	0.5918	0.0964
Duration	0.70	0.55	0.65	0.50	0.0063	0.900	0.001	0.001
Pitch	-0.43	14.65	4.86	16.50	0.00079	0.0045	0.001	0.001
Angular velocity	-4.06	4.10	-4.53	5.41	0.001	0.7341	0.4721	0.0705
Bout								
Peak speed	14.27	7.61	13.45	8.79	0.09274	0.900	0.0501	0.536
Trajectory	-1.47	17.85	4.02	21.39	0.5466	0.017	0.001	0.001
Vertical displacement (climb)	0.19	0.24	0.21	0.29	0.01468	0.88274	0.00107	0.00001
Vertical displacement (dive)	-0.23	0.21	-0.21	0.24	0.0807	0.63421	0.04238	0.00082
Attack angle (climb)	1.87	4.07	1.63	4.49 8	0.01707	0.35229	0.001	0.0875
Attack angle (dive)	-2.45	4.02	-4.25	5.06	0.13825	0.70259	0.001	0.002
Steering rotation gain	0.76		0.72		0.04204	0.09151	0.0263	0.6869
Righting rotation gain	0.09		0.10		0.81049	0.25570	0.001	0.001

Table 5: Pre-treatment results for light-dark dataset. P-value calculated using unpaired t-test (alpha = 0.05).

Parameter	Unit of Measure	Control Median	Control IQR	Copper Median	Copper IQR	P-Value
Inter-bout intervals						
Vertical displ	mm	-0.09	0.20	-0.08	0.22	0.33009
Vertical velocity	mm/s	-0.16	0.23	-0.14	0.21	0.39788
Duration	s	0.62	0.35	0.66	0.43	0.71332
Pitch	deg	0.08	15.03	0.62	15.60	0.82852
Angular velocity	deg/s	-2.21	3.86	-1.98	3.54	0.56789
Bouts						
Peak speed	mm/s	12.41	7.07	11.92	6.53	0.52552
Trajectory	deg	-0.36	18.18	0.07	18.78	0.92503
Vertical displ (climb)	mm	0.17	0.21	0.17	0.22	0.88274
Vertical displ (dive)	mm	-0.18	0.18	-0.16	0.17	0.63421
Attack angle (climb)	deg	2.28	3.75	2.10	3.50	0.35229
Attack angle (dive)	deg	-1.86	3.20	-2.09	3.21	0.70259
Steering rotation gain		0.74		0.75		0.54368
Righting rotation gain		0.08		0.07		0.31203

Table 6: Navigational make-up of swim bouts after copper treatment.

Light	Condition	Climb bouts	Flat bouts	Dive bouts	Total bouts	Climb %	Flat %	Dive %
Dark-Dark	control	11123	10795	10795	32713	33	33	33
Dark-Dark	copper	4822	4797	3507	13126	37	36	27
Light-Dark	control	58951	57217	57218	173386	34	33	33
Light-Dark	copper	58758	31903	27743	118404	50	27	23

SUPPLEMENTAL VIDEO

Video S1

Video S1. Real-time recording of control and copper-treated larvae after treatment. Notably, copper-treated larvae sink between bouts, while controls maintain their position in depth. Related to Figure 2.